# Electronic, Magnetic, and Spectroscopic Properties of Binuclear Diruthenium Tetracarboxylates: A Theoretical and Experimental Study

**Guillermina Estiú,*,† Fabio D. Cukiernik,*,‡ Pascale Maldivi,§,|| and Olivier Poizat⊥**

CEQUINOR, Departamento de Química, Facultad de Ciencias Exactas, Universidad Nacional de la Plata, CC 962, La Plata (1900) Argentina, INQUIMAE, Departamento de Química Inorgánica, Analítica y Química Física, Facultad de Ciencias Exactas y Naturales, Universidad de Buenos Aires, Pabellón II, Ciudad Universitaria, Núñez, 1428 Capital Federal, Argentina, Instituto de Ciencias, Universidad Nacional de General Sarmiento, Roca 850, 1663 San Miguel, Buenos Aires, Argentina, Laboratoire de Chimie de Coordination, Service de Chimie Inorganique et Biologique, Département de Recherche Fondamentale sur la Matière Condensée, CEA/Grenoble, 17 Rue des Martyrs, 38054 Grenoble, France, and Laboratoire de Spectrochimie Infrarouge et Raman, CNRS, 2 Rue Henri Dunant, 94320 Thiais, France

*Received September 10, 1998*

The electronic structure of binuclear diruthenium tetracarboxylates, in both the divalent $Ru_2^{II,II}(O_2CR)_4$ and the mixed-valent $Ru_2^{II,III}(O_2CR)_4X$ (X = anion) states is studied by means of ZINDO/S-MRCI and DFT calculations. Both methods predict a $(\pi^*)^2(\delta^*)^2$ ground-state configuration for the divalent species, contrary to the $(\pi^*)^3(\delta^*)^1$ previously predicted by SCF-X$\alpha$ calculations, but in agreement with magnetic measurements that show a strong Zero Field Splitting. Our ZINDO/S-MRCI calculations on compounds containing axial ligands with different degree of $\pi$ bonding to the bimetallic center (water, chloride, carboxylate, pyridine, pyrazine), for both (II,II) and (II,III) ruthenium cores, show the important role played by the ligands. These theoretical calculations allow us to explain the differences observed in the UV/vis and resonance Raman spectra, both in solution and in the solid state, when varying the axial ligands. The ZINDO/S-MRCI calculations are also capable of solving some controversies found in the literature, related to the assignment of the main electronic bands for both kinds of compounds. The electronic structures predicted by the DFT methodology are in agreement with both the experimental evidence and the ZINDO/S calculations. Moreover, our DFT calculations provide an interpretation of the intermolecular magnetic interactions in the mixed-valent species, explaining the dependence of the antiferromagnetic coupling on the intermolecular Ru−X−Ru angle.

## Introduction

Dimeric ruthenium tetracarboxylates have been the focus of both theoretical and experimental studies since the pioneering works of Wilkinson[1] and Cotton.[2] However, because of their potential applications, the research interest in these compounds has increased significantly in recent years.[3] From an inorganic chemistry standpoint, the main interest is related to the multiple metal−metal bonds (MMMB) and paramagnetic ground states that characterize both the divalent $Ru_2^{II,II}(RCO_2)_4$ and mixed-valent $Ru_2^{II,III}(RCO_2)_4X$ (X = anion) species. Multiple bonds have been largely analyzed in bimetallic species in connection with the relative effects of axial and equatorial-bridging ligation on the bond length. The magnetic properties, on the other hand, have challenged the researchers for many years, since the classical MO description of MMMB[2,4,5] has not been able to offer an interpretation for their room-temperature magnetic moment. From a materials chemistry point of view, these carboxylates are of importance thanks to their physical properties,[3] that make them suitable candidates for the design of advanced molecular materials, such as their liquid crystalline character[6] and magnetic properties.[6a,c,7]

To better understand, and even control, those collective properties, it seems useful to get a deeper insight into both the

† CEQUINOR.
‡ INQUIMAE and ICI-UNGS.
§ CEA Grenoble.
|| Present adress: Laboratoire de Reconnaissance Ionique, Service de Chimie Inorganique et Biologique/DRFMC, CEA-Grenoble, 17 Rue des Martyrs, 38054 Grenoble Cedex 9, France.
⊥ CNRS.

(1) Stephenson, T. A.; Wilkinson, G. J. *J. Inorg. Nucl. Chem.* **1966**, *8*, 2285.
(2) Bennet, M. J.; Caulton, K. G.; Cotton, F. A. *Inorg. Chem.* **1969**, *8*, 1.
(3) For a recent review, see: Aquino, M. A. S. *Coord. Chem. Rev.* **1998**, *170*, 141.
(4) Cotton, F. A., Walton, R. A. *Multiple Bonds between Metal Atoms*; John Wiley & Sons: New York, 1982.
(5) Norman, J. G.; Renzoni, G. E.; Case, D. A. *J. Am. Chem. Soc.* **1979**, *101*, 5256.
(6) (a) Maldivi, P.; Giroud-Godquin, A. M.; Marchon, J. C.; Guillon, D.; Skoulios, A. *Chem. Phys. Lett.* **1989**, *157*, 552. (b) Cukiernik, F. D.; Maldivi, P.; Giroud-Godquin, A. M.; Marchon, J. C.; Ibn-Elhaj, M.; Guillon, D.; Skoulios, A. *Liq. Cryst.* **1991**, *9*, 903. (c) Bonnet, L.; Cukiernik, F. D.; Maldivi, P.; Giroud-Godquin, A. M.; Marchon, J. C.; Ibn-Elhaj, M.; Guillon, D.; Skoulios, A. *Chem. Mater.* **1994**, *6*, 31. (d) Cukiernik, F. D.; Ibn-Elhaj, M.; Chaia, Z. D.; Marchon, J. C.; Giroud-Godquin, A. M.; Guillon, D.; Skoulios, A.; Maldivi, P. *Chem. Mater.* **1998**, *10*, 83. (e) Cayton, R. H.; Chisholm, M. H.; Darrington, F. D. *Angew. Chem., Int. Ed. Engl.* **1990**, *29*, 1481. (f) Baxter, D. V.; Cayton, R. H.; Chisholm, M. H.; Huffman, J. C.; Putilina, E. F.; Tagg, S. L.; Wesemann, J. L.; Zwanziger, J. W.; Darrington, F. D. *J. Am. Chem. Soc.* **1994**, *116*, 4551. (g) Caplan, J. F.; Murphy, C. A.; Lemieux, R. P., Cameron, S. T., Aquino, M. A. S. *Can. J. Chem.* **1998**, *76*, 1520.

10.1021/ic981098+ CCC: $18.00 
Published on Web 06/11/1999

electronic structure of the individual dimers, and the influence of the supramolecular structure. Such issues have not yet been completely resolved.[3,8,9]

The electronic characteristics of the individual dimers are nicely reflected in their magnetic behavior, which shows the presence of 3 and 2 unpaired electrons for the (II,III) and (II,II) compounds, respectively.[1,6,7,10] This fact was first interpreted by Norman, Renzoni, and Case (NRC)[5] on the basis of their Xα calculations. They proposed a $(\pi^*)^2(\delta^*)^1$ configuration as the ground state for the mixed-valent compounds, and a $(\pi^*)^3(\delta^*)^1$ configuration for the ground state of the divalent analogues. In the latter, an excited $(\pi^*)^2(\delta^*)^2$ configuration was located 2 kcal/mol higher in energy, according to the calculations performed by these authors.

Spectroscopy has played an important role in the analysis of the electronic structure of these compounds.[11] Detailed UV/vis, far-IR, and RR experiments[11a−d] have led to conclusions that are in agreement with the electronic structure proposed by Norman et al. for the mixed-valent systems. However, the interpretation of the photoelectron spectra of the (II,II) complexes, based on ab initio calculations,[11e] indicates that a $(\pi^*)^2(\delta^*)^2$ configuration associated with the ground state is 15 kcal/mol lower in energy than the $(\pi^*)^3(\delta^*)^1$ state. Even if this theoretical conclusion is not very well supported, as only the first state has been corrected by means of the adition of Generalized Valence Bond pairs, further experimental results supported a $(\pi^*)^2(\delta^*)^2$ ground-state configuration. Indeed, magnetic measurements, carried out on a wide temperature range, have shown the presence of a very strong zero-field splitting (ZFS) in both the divalent[6a,7,12] and the mixed-valent[7a−d,g] systems. Cotton et al have shown[12] that the ZFS of the (II,II) compounds could not arise from the $^3$E term of a $(\pi^*)^3(\delta^*)^1$ configuration, giving further support to a ground-state assignment compatible with a $(\pi^*)^2(\delta^*)^2$ electron distribution. Furthermore, it has been shown later that a $(\pi^*)^2(\delta^*)^2$ configuration is more consistent with the molecular structural data.[12a,13]

It follows from the previous discussion that the subject is still a matter of investigation. Numerous experimental studies (mainly magnetic and spectroscopic measurements) were carried out in the past in order to understand the electronic structure of these species.[6a,7a,b,11] Moreover, several research groups are currently investigating the spectroscopic properties of these compounds both in solution[8,13,14] and in the solid state[7c−g,8,14]

The research presented in this article has the aim of understanding, at a molecular level, the electronic processes that govern the observed properties of both the mixed-valent and divalent diruthenium tetracarboxylates, by means of the use of combined theoretical and experimental approaches. The results of our quantum chemical calculations performed at the semiempirical ZINDO/S-MRCI and DFT levels offer an interpretation of their physical behavior in both the solid phase and in solution. Although the necessity of theoretical calculations to help understand these systems has been largely claimed,[8,10h,12b] we are not aware of previous published studies at this level of correlation. As a way of validating their accuracy, the results have been compared to those obtained from Xα, ab initio calculations, and experimental measurements, whenever available.

## Calculations and Experimental Procedures

**(a) ZINDO/S-MRCI Calculations.** We apply the intermediate neglect of differential overlap (INDO) model[15−17] at the self-consistent field multireference configuration interaction (SCF/MRCI) level to study the electronic characteristics, magnetic properties and spectroscopy of divalent and mixed valent ruthenium tetracarboxylates. The parametrization of the method that we are using (ZINDO/S)[18−20] obtains the two-center two-electron integrals from atomic spectroscopy at the MRCI singles (MRCIS) level, and is, therefore, highly reliable for the study of UV/visible spectroscopy. Because it is parametrized on electronic grounds, it affords a very accurate determination of the most stable electronic configuration and multiplicity (M), together with the associated electronic and magnetic characteristics of a given structure.

The orbitals that define the basis for the MRCI studies are obtained from calculations at either a RHF or a ROHF level, depending on the characteristics of the structure under study. Special care has been taken not to destroy the orbital symmetry during the SCF cycles, an effect that can occur through a nonequivalent occupation of degenerate orbitals. The orbitals obtained carelessly do not represent the actual state of the molecule to which they belong. To avoid these errors, calculations are started by a configuration average Hartree−Fock (CAHF)[21] procedure with an average M for the number of electrons considered. The number of orbitals included in the average are decreased in consecutive cycles, up to a minimal set that retains an accurate definition of closed and open shell operators in agreement with the symmetry of the compounds. Those are the basis for a further RHF or

(7) (a) Telser, J.; Drago, R. S. *Inorg. Chem.* **1984**, *23*, 3114. (b) Telser, J.; Miskowsky, V. M.; Drago, R. S.; Wong, N. M. *Inorg. Chem.* **1985**, *24*, 4765. (c) Cukiernik, F. D.; Giroud-Godquin, A. M.; Maldivi, P.; Marchon, J. C. *Inorg. Chim. Acta* **1994**, *215*, 203. (d) Cukiernik, F. D.; Luneau, D.; Marchon, J. C.; Maldivi, P. *Inorg. Chem.* **1998**, *37*, 3698. (e) Cotton, F. A.; Kim, Y.; Ren, T. *Inorg. Chem.* **1992**, *31*, 2608. (f) Cotton, F. A.; Kim, Y.; Ren, T. *Inorg. Chem.* **1992**, *31*, 2723. (g) Beck, E. J.; Drysdale, K. D.; Thompson, L. K.; Li, L.; Murphy, C. A.; Aquino, M. A. S. *Inorg. Chim. Acta* **1998**, *279*, 121.

(8) Drysdale, K. D.; Beck, E. J.; Cameron, T. S.; Robertson, K. N.; Aquino, M. A. S. *Inorg. Chim. Acta* **1997**, *256*, 243.

(9) (a) As an example, an inorganic journal did not include any paper on diruthenium systems in a special issue devoted to the theoretical treatement of metal−metal bonded systems. *Polyhedron* **1987**, *6*. (b) Some recent work on DFT applied to multiple metal−metal bonded systems have not treated ruthenium compounds: Cotton, F. A.; Feng, X. *J. Am. Chem. Soc.* **1997**, *119*, 7514. Cotton, F. A.; Feng, X. *J. Am. Chem. Soc.* **1998**, *120*, 3387.

(10) (a) Togano, T.; Mukaida, M.; Nomura, T. *Bull. Chem. Soc. Jpn.* **1980**, *53*, 2085. (b) Lindsay, A. J.; Tooze, R. P.; Motevalli, M.; Hursthouse, M. B.; Wilkinson, G. *J. Chem. Soc. Chem. Commun.* **1984**, 1383. (c) Mukaida, M.; Nomura, T.; Ishimori, T. *Bull. Chem. Soc. Jpn.* **1972**, *45*, 2143. (d) Das, B. K.; Chakravarty, A. R. *Polyhedron* **1988**, *7*, 685. (e) Barral, M. C.; Jiménez-Aparicio, R. Rial, C.; Royer, E.; Saucedo, M. J.; Urbanos, F. A. *Polyhedron* **1990**, *9*, 1723. (f) Higgins, P.; McCann, M. *J. Chem. Soc., Dalton Trans.* **1988**, 661. (g) Carvill, A.; Higgins, P.; McCann, M.; Ryan, H.; Shiels, A. *J. Chem. Soc., Dalton Trans.* **1989**, 2435. (h) Lindsay, A. J.; Wilkinson, G.; Motevalli, M.; Hursthouse, M. B. *J. Chem. Soc., Dalton Trans.* **1985**, 2321. (i) Lindsay, A. J.; Wilkinson, G.; Motevalli, M.; Hursthouse, M. B. *J. Chem. Soc., Dalton Trans.* **1987**, 2723.

(11) (a) Martin, D. S.; Newman, R. A.; Vlasnik, L. S. *Inorg. Chem.* **1980**, *19*, 3404. (b) Clark, R. J. H.; Ferris, L. T. H. *Inorg. Chem.* **1981**, *20*, 2759. (c) Miskowski, V. M.; Loehr, T. M.; Gray, H. B. *Inorg. Chem.* **1987**, *26*, 1098. (d) Miskowski, V. M.; Gray, H. B. *Inorg. Chem.* **1988**, *27*, 2501. (e) Quelch, G. E.; Hillier, I. H.: Guest, M. F. *J. Chem. Soc., Dalton Trans.* **1990**, 3075.

(12) (a) Cotton, F. A.; Miskowski, V. M.; Zhong, B. *J. Am. Chem. Soc.* **1989**, *111*, 6177. (b) Cotton, F. A.; Ren, T.; Eglin, J. L. *Inorg. Chem.* **1991**, *30*, 2552.

(13) Chisholm, M. H.; Christou, G.; Folting, K.; Huffman, J. C.; James, C. A.; Samuels, J. A.; Wesemann, J. L.; Woodruff, W. H. *Inorg. Chem.* **1996**, *35*, 3643.

(14) Cukiernik, F. D. Ph.D. Thesis. University of Grenoble, 1993.

(15) Pople, J. A.; Santry, D. P.; Segal, G. A.; *J. Chem. Phys.* **1965**, *43*, S129.

(16) Pople, J. A.; Beveridge, D. L.; Dobosh, P. A.; *J. Chem. Phys.* **1967**, *47*, 47.

(17) Zerner, M. C. *ZINDO Package*; Quantum Theory Project; Williamson Hall, University of Florida: Gainesville, FL, Version 1998.

(18) Ridley, J.; Zerner, M. C. *Theor. Chim. Acta* **1973**, *32*, 111.

(19) Ridley, J.; Zerner, M. C. *Theor. Chim. Acta* **1976**, *42*, 223.

(20) Zerner, M. C.; Loew, G.; Kirchner, R.; Mueller-Westerhoff, U. *J. Am. Chem. Soc.* **1980**, *102*, 589.

(21) Zerner, M. C. *Int. J. Quantum Chem.* **1989**, *35*, 567.

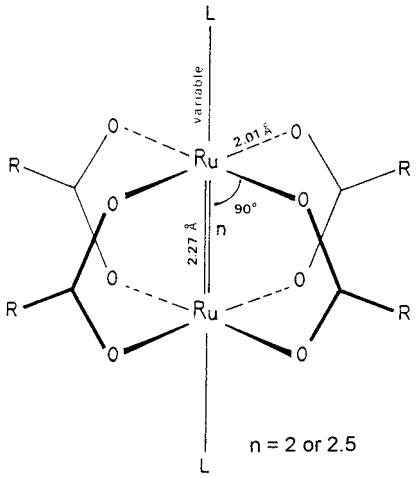


**Figure 1.** Molecular geometry and average parameters used for the calculations

ROHF calculation. A Rumer[22] MRCI calculation, using the eigenvectors from the last cycle, follows this procedure. When dealing with electronic spectra, the intensity of the bands is expressed by means of their oscillator strengths, evaluated with the dipole-length operator,[23] retaining all one-center terms. The details of the MRCI calculations, regarding the number of references, size of the MRCI space and symmetry imposed to the calculation, depends on the size and the geometry of the system under study and are discussed, for each particular case, in the next section.

The coordinates for $Ru(O_2CH)_4$, $Ru(O_2CH)_4^+$, and their diaqua derivatives (Figure 1) have been derived from the average crystallographic bond parameters of more than 20 compounds (collected in ref 14). The Ru−N distance, as well as the orientation of the cycles relative to the carboxylates of the central core, for the compounds with axial pyrazine and pyridine ligands also comes from crystallographic determinations.[7e,f] All the other parameters have been taken from the data collected in ref 14.

In all the cases the bridging groups were simplified to their $O_2CH$ analogues. The geometries of the complexes were idealized to $D_{4h}$, $D_{2h}$, or $C_{2v}$ symmetry whenever possible. The axial substituents were defined in the plane of the carboxylates, except for the pyridine cycle, which is known to lie between them and was modeled defining a 45° angle. No geometry optimization has been performed, as we are not interested in isolated monomer structures but in those built either in the solid phase or in coordinating or noncoordinating solvents, for which experimental data define more accurate models.

**(b) DFT Calculations.** The DFT computations have been carried out with the Amsterdam Density Functional package (ADF 2.3).[24] Core electron densities are kept frozen, in a [He] core for C, N, and O, a [Ne] core for Cl, and a [Kr] core for Ru. The valence basis sets are triple-$\zeta$ Slater functions in the case of Ru and one d polarization function was added for all other atoms. The exchange and correlation potentials were self-consistently corrected within the generalized gradient approximation (GGA) with the non local exchange functional of Becke[25] and the correlation part of Perdew.[26] The unrestricted SCF computations were spin polarized with $S_z = 2$ (number of $\alpha$ electrons minus number of $\beta$ electrons) for the divalent species, $S_z = 3$ for mixed-valent systems and $S_z = 6$ for the "dimer of dimers" $[Ru_2(O_2CH)_4{-}Cl{-}Ru_2(O_2CH)_4]^+$.

The structural features of the systems have been described above (see part a). The model system $[Ru_2(O_2CH)_4{-}Cl{-}Ru_2(O_2CH)_4]^+$ was derived from the cristallographic structure of the chloro-pentanoate derivative,[7d] replacing the $C_3H_7$ groups by H, and varying the Ru−Cl−Ru angle (see below).

**(c) Experimental Section.** All the studied compounds were synthesized following literature methods.[6c,d,14,27] UV/visible spectra were measured on a Perkin-Elmer Lambda 9 spectrometer (solid spectra were obtained with Nujoll mulls between glass plates). The resonance Raman experiments were performed with a Dilor RTI 30 triple monochromator spectrometer, as well as with a microspectrometer Dilor XY equipped with a CCD Wright detector refrigerated with liquid $N_2$. To improve the signals (reducing autoabsorption), the powdered products were diluted (1:30 to 1:100) in KBr. The sample temperature was controlled with a homemade cryostat.

## Results and Discussion

**Divalent Compounds. (a) (1) Electronic Structure: ZINDO Calculations.** The electronic molecular orbital (MO) distribution of the compounds of general formula $M_2(O_2CR)_4$ has been the subject of numerous quantum chemical analysis. It has been demonstrated by several spectroscopic techniques that the MO distribution of dimetal tetracarboxylates, in either coordinating or noncoordinating media, is influenced by the nature of the axial ligands,[8,11c,13,14] which will modify the electronic characteristics of the M−M bond itself and, through them, its geometric characteristics. However, because of their simplicity, axially free compounds have been the first to be studied. For the case of the Ru(II) carboxylates $[Ru_2^{II,II}(O_2CR)_4]$, the traditional $\sigma\pi\delta\delta^*\pi^*\sigma^*$ description of the MO ordering derived from the concepts of the metal−metal bond, is not so obvious, as the d orbital splitting will depend on the respective strength of the M ligand and M−M interactions, which are, on the other hand, mutually interconnected. Because the $\delta^*$ and the $\pi^*$ antibonding orbitals lie very close in energy, they can be both occupied in the $Ru_2^{n+}$ units[5,11e] and can give rise to different configurations, which are determined, in part, by the ligands involved. Moreover, it should be kept in mind, as Chisholm has pointed out before,[13] that the ground state for the unligated $Ru_2(O_2CR)_4$ species has been theoretically analyzed using metric parameters taken for ligated compounds, and the conclusions are, therefore, approximated.

Throughout this discussion, we will compare our results to those of NRC. These authors have found a $\sigma\pi\delta\pi^*\delta^*\sigma^*$ configuration for both the axially free and water coordinated compounds, with a $\delta^*\pi^*$ inversion derived from the more efficient destabilization of the $\delta^*$ orbitals through antibonding interactions with the $1b_u$ ($D_{4h}$ symmetry) of the carboxylate groups. In agreement with NRC, we have also found that for the axially free compound the $\delta^*$ is destabilized above the $\pi^*$ to give a final electronic configuration $\sigma\pi\delta\pi^*\delta^*\sigma^*$, as shown in Figure 2. For this MO distribution the experimentally found triplet state can be assigned to a $(\pi^*)^2(\delta^*)^2$ configuration. However, our MRCI calculations, indicate that the $\sigma^*$ orbital is also occupied, to give a quintet ground state, associated with a $(\pi^*)^2(\delta^*)^1(\sigma^*)^1$ configuration, with a bond order equal to 2. The triplet $(\pi^*)^2(\delta^*)^2$ is calculated 0.024 au higher in energy (details on the calculation and other excited states are given in Table 1). Although this result seems to be at variance with the experimental evidence, it should be kept in mind that the experiments do not deal with isolated cores. Even for the best noncoordinating media the dimetal cores are probably part of oligomer chainlike structures. Chisholm has recently found a significant difference in the $^1H$ NMR of a Ru(II,II) tetracarboxylate when it is measured in coordinating and noncoordinating media,[13] which has been explained on the basis of the presence of such oligomeric species.

(22) Pauncz, R. *Spin Eigenfunctions*; Plenum: New York, 1979.
(23) Cory, M. G.; Zerner, M. C. *Chem. Rev.* **1991**, *91*, 1, 813.
(24) (a) *ADF 2.3.0*; Theoretical Chemistry, Vrije Universiteit: Amsterdam, The Netherlands. (b) Baerends, E. J.; Ellis, D. E.; Ros, P. *Chem. Phys.* **1973**, *2*, 41. (c) te Velde, G.; Baerends, E. J. *J. Comput. Phys.* **1992**, *99*, 84.
(25) Becke, A. D. *Phys. Rev. A.* **1988**, *38*, 3098.
(26) Perdew, J. P. *Phys. Rev. B.* **1986**, *33*, 8822.
(27) (a) Mitchell, R. W.; Spencer, A.; Wilkinson, G. *J. Chem. Soc., Dalton Trans.* **1973**, 846. (b) Forest, E.; Maldivi, P.; Marchon, J. C.; Virelizier, H. *Spectroscopy* **1987**, *5*, 129.

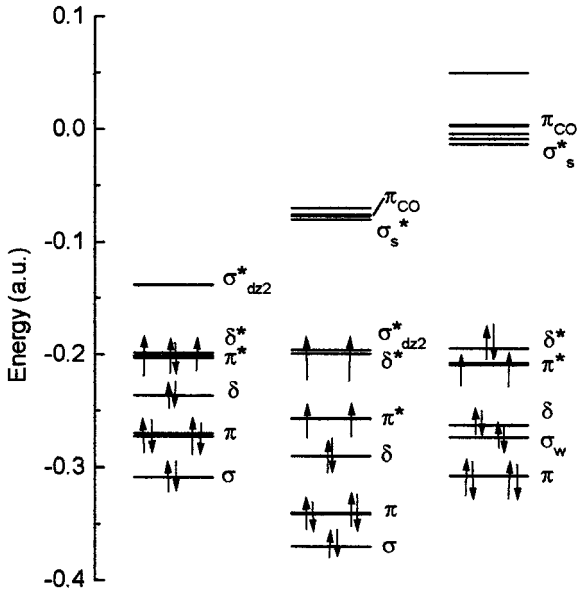


**Figure 2.** Molecular orbital diagrams for divalent $Ru_2(O_2CH)_4$, as calculated by Xα (left, after ref 4) and ZINDO/S-MRCI (middle) as well as for $Ru_2(O_2CH)_4(H_2O)_2$ (right) from ZINDO/S-MRCI calculations (eigenvalues in au). Only MO's with high metal contributions have been represented.

**(2) Influence of the Axial Ligands.** The modeling of coordinated solvent (as well as solid $Ru_2(O_2CR)_4L_2$ complexes), through the definition of two axially bonded water molecules, generates a significant change in the MO distribution of the complexes (Figure 2), in both the fundamental and excited configurations (see Table 1). According to the ZINDO calculations, the interaction of the $3a_1$ orbitals of the ligand with the $d_{z^2}$ of the Ru destabilizes the $\sigma^*_{d_{z^2}}$ orbital which, lying above the $\pi^*$ and $\delta^*$, gives a $\pi\sigma_w\delta\pi^*\delta^*\sigma^*$ ($\sigma_w$ = bonding combination $\sigma^*_{d_{z^2}}$−water) electronic distribution. MRCI calculations (Table 1) result in a triplet $(\pi^*)^2(\delta^*)^2$ ground state for the diaquo complex. Axially bonded water molecules decrease the symmetry of the molecule from $D_{4h}$ to $D_{2h}$. It should be kept in mind that we are referring, in our discussion, to the idealized $D_{4h}$ geometry. The actual symmetry is lower. Although there are no degenerate orbitals in $D_{2h}$ symmetry, we refer to the $d_{xz}$, $d_{yz}$ orbitals on the Ru atoms as $\pi$, to make feasible their comparison with the axially free compounds. These orbitals are, on the other hand, almost degenerate.

To better confirm the importance of the axial ligands in the definition of the electronic configuration of diruthenium(II,II) carboxylates, we have analyzed the influence of the distance of these ligands to the central ruthenium core. To this end, the Ru−O distance has been changed in 0.1 Å steps from its equilibrium up to a value Ru−O = 3.7 Å, a distance for which the system is described as two isolated water molecules and the central core. The first effect that becomes evident as the water molecules are getting farther is the recovery of the degeneracy of the $\pi$ orbital, which becomes effective for a 0.2 Å shift of the ligands. The second effect is associated with the relative order of the molecular orbitals. For the water molecules separated 0.8 Å from their equilibrium position, the $\sigma^*_{d_{z^2}}$−$\sigma^*_s$ orbitals are interchanged, and for a 1.2 Å displacement, the MO distribution of the axially free molecule has been reestablished. For this distance, and this orbital distribution, $M = 5$ is preferred after the MRCI calculations.

The effect of $\pi$ coordinating axially bonded ligands, like pyrazine, on the divalent central core is similar to that previously described for water ligands. The $\sigma^*_{d_{z^2}}$ orbital of the Ru atoms is pushed up in energy through antibonding interactions with the nitrogen $p_z$ of the pyridine cycle. The MO distribution that we calculate is similar to the one found for the complex with water ligands, with a small change in the ordering of the bonding orbital defined by the $\sigma$, which lies above the $\delta$ due to its more effective interaction with the nitrogen $p_z$. Both the $\pi$ and $\pi^*$ ruthenium orbitals are delocalized in the $\pi$ system of the pyrazine ligands. The final electronic configuration is, therefore, $\pi\delta\sigma_{p_z}\pi^*\delta^*\sigma^*$ ($\sigma_{p_z}$ = bonding combination $\sigma^*_{d_{z^2}}$−$p_z$; $\sigma^*$ = antibonding combination $\sigma_{d_{z^2}}$−$p_z$).

Our MRCI calculations (see Table 1) shows that the ground state is a triplet $(\pi^*)^2(\delta^*)^2$. The excited $M = 3$ state is actually composed by two nearly degenerate states, separated 0.004 au, which are split through interactions with the $\pi$ system of the pyrazine ligands, an effect that increases the lack of degeneracy of the ($\pi^*$) orbitals under $D_{2h}$ symmetry. The quintuplet, associated with the promotion of one electron to the nitrogen $p_z$ on the pyrazine moiety, is calculated 0.049 au above the most stable triplet.

**(b) Electronic Structure: DFT Calculations.** The MO schemes derived from DFT calculations are represented in Figure 3 for $Ru_2(O_2CH)_4$ and the bis-adducts with $H_2O$ and pyridine in axial positions. In the three species, the antibonding MO's $\pi^*$ and $\delta^*$ are in the appropriate order (as expected by theoretical[12b] and molecular structures[12a,13] observations) to yield a $(\pi^*)^2(\delta^*)^2$ ground electron configuration. The $(\pi^*)^3(\delta^*)^1$ triplet configuration is 0.012 au above the latter in the case of the noncoordinated species. In all cases, the $\sigma^*$(Ru−Ru) is higher in energy than the antibonding MO's $\pi^*$ and $\delta^*$, with an upward shift of this MO, for the axially ligated species, compared to $Ru_2(O_2CH)_4$. The $\sigma$(Ru−$L_{ax}$) orbital is located between the $\pi$ and $\delta$ orbitals in the case of L = $H_2O$ and above the $\delta$ level for the L = pyridine system. It should also be noted that some $\pi$-back-bonding occurs in the case of the pyridine adduct, leading to a small amount of mixing between the $\pi^*$-(Ru−Ru) and a vacant $\pi^*$ of the aromatic rings. This description is in agreement with the one derived from the MRCI calculations.

**(c) Comparison of the Results of ZINDO/S-MRCI and DFT Methodologies.** Both methods predict similar MO distributions (as seen by comparing Figures 2 and 3), as well as similar ground states for the (II,II) compounds analyzed. The only exception to this agreement is related to the prediction of the ground state of the unsolvated species, $Ru_2(O_2CH)_4$. The small energy difference between the $\delta^*$ and $\pi^*$ orbitals (0.0055 au) can justify this discrepancy, as the result is dependent on the degree of electron correlation included in the calculation. Moreover, the relative position of the $\pi^*$ and $\delta^*$ orbitals depends on the strength of the Ru−Ru interaction. Taking into account the different sensitivity of the different methodologies to structural parameters, slight geometry changes might lead to different results. On this basis, dealing with a hypothetical compound of unknown structure, the reliability of the different approaches cannot be judged.

We conclude, from the previous discussion, that axial interactions should be considered, in both coordinating and noncoordinating media, to reproduce the experimental data. Whereas in coordinating media the axial sites are occupied by solvent molecules, in noncoordinating media oligomers (whose electronic structure and properties will also resemble those of ligated species) are formed via axial interaction. This conclusion is consistent with the one derived by Chisholm[13] from the experimental investigation of the effect of ligation to the $Ru_2$ core.

**Table 1.** Results and Details of the ZINDO/S-MRCI Calculations for the Different Ru Compounds[a]

| Compound | MRCI space oc | MRCI space v | no. of reference states | no. of configurations | MO distribution | b.o. | calculated states config. | calculated states $\Delta E$(au) | calculated states $M$ |
|---|---|---|---|---|---|---|---|---|---|
| $Ru_2(O_2CH)_4$ | 13 | 6 | 3 | 277 | $\sigma\pi\delta\pi^*\delta^*\sigma^*_{d_z^2}\sigma^*_s$ | 2 | $(\pi^*)^2(\delta^*)^2$ | 0.04 | 1 |
| | | | 1 | 335 | | | $(\pi^*)^2(\delta^*)^2$ | 0.024 | 3 |
| | | | 1 | 284 | | | $(\pi^*)^2(\delta^*)^1(\sigma^*)^1$ | 0.00 | 5 |
| $Ru_2(O_2CH)_4(H_2O)_2$ | 11 | 8 | 4 | 380 | $\sigma\pi\sigma_w\delta\pi^*\delta^*\sigma^*_s\sigma^*_{d_z^2}$ | 2 | $(\pi^*)^2(\delta^*)^2$ | 0.017 | 1 |
| | | | 3 | 570 | | | $(\pi^*)^2(\delta^*)^2$ | 0.00 | 3 |
| | | | 2 | 408 | | | $(\pi^*)^2(\delta^*)^1(\sigma^*)^1$ | 0.08 | 5 |
| $Ru_2(O_2CH)_4(pz)_2$ | 20 | 15 | 4 | 247 | $\sigma\pi\delta\sigma_{p_z}\pi^*\delta^*\sigma^*$ | 2 | $(\pi^*)^3(\delta^*)^1$ | 0.0018 | 1 |
| | | | 3 | 1280 | | | $(\pi^*)^3(\delta^*)^1$ | 0.002 | 3 |
| | | | 3 | 1280 | | | $(\pi^*)^2(\delta^*)^2$ | 0.000 | 3 |
| | | | 1 | 960 | | | $(\pi^*)^3(\delta^*)^1\sigma^*$ | 0.049 | 5 |
| $[Ru_2(O_2CH)_4]^+$ | 12 | 6 | 3 | 672 | $\sigma\pi\delta\ \pi^*\delta^*\sigma^*$ | 2.5 | $(\pi^*)^3$ | 0.013 | 2 |
| | | | 1 | 296 | | | $(\pi^*)^2(\delta^*)^1$ | 0.00 | 4 |
| | | | 1 | 352 | | | $\delta\ (\pi^*)^2(\delta^*)^1\sigma^*$ | 0.04 | 6 |
| $[Ru_2(O_2CH)_4Cl_2]^-$ | 12 | 7 | 3 | 690 | $\sigma\pi\delta\ \pi^*\delta^*\sigma^*$ | 2.5 | $(\pi^*)^3$ | 0.03 | 2 |
| | | | 2 | 304 | | | $(\pi^*)^2(\delta^*)^1$ | 0.036 | 2 |
| | | | 2 | | | | $(\pi^*)^2(\delta^*)^1$ | 0.000 | 4 |
| | | | 2 | 360 | | | $\delta(\pi^*)^2(\delta^*)^1(\sigma_*^*)^1$ | 0.11 | 6 |
| $[Ru_2(O_2CH)_4(H_2O)_2]^+$ | 12 | 10 | 3 | 620 | $\pi\sigma\delta\pi^*\delta^*\sigma^*_s\sigma^*_{d_z^2}$ | 2.5 | $(\pi^*)^2(\delta^*)^1$ | 0.02 | 2 |
| | | | 1 | 244 | | | $(\pi^*)^2(\delta^*)^1$ | 0.00 | 4 |
| | | | 1 | 494 | | | $\delta(\pi^*)^2(\delta^*)^1(\sigma_{d_z^2}^*)$ | 0.15 | 6 |
| $[Ru_2(O_2CH)_4(pz)_2]^+$ | 6 | 6 | 3 | 615 | $\pi\delta\sigma_{p_z}\delta^*\pi^*\sigma^*_s\sigma^*_{d_z^2}$ | 2.5 | $(\delta^*)^1(\pi^*)^2$ | 0.02 | 2 |
| | | | 1 | 251 | | | $(\delta^*)^1(\pi^*)^2$ | 0.00 | 4 |
| | | | 3 | 515 | | | $(\sigma_{p_z})^1(\delta^*)^1(\pi^*)^2(\sigma_{d_z^2}^*)^1$ | 0.1 | 6 |
| $[Ru_2(O_2CH)_6]^-$ | 6 | 6 | 3 | 484 | $\pi\delta\sigma_{d_z^2}\delta^*\pi^*\sigma^*_s\sigma^*_{d_z^2}$ | 2.5 | $(\delta^*)^1(\pi^*)^2$ | 0.024 | 2 |
| | | | 3 | | | | $(\delta^*)^2(\pi^*)^1$ | 0.026 | 2 |
| | | | 1 | 203 | | | $(\delta^*)^1(\pi^*)^2$ | 0.000 | 4 |
| | | | 2 | 267 | | | $(\sigma_{d_z^2})^1(\delta^*)^1(\pi^*)^2(\sigma_{d_z^2}^*)$ | 0.80 | 6 |

[a] The data has to be read as follows: for example, for $Ru_2(O_2CH)_4(H_2O)_2$, MRCI calculations, including 4, 3, and 2 references and a MRCI space defined by 11 orbitals down and 8 up the Fermi level, leading to 380, 570, and 408 configurations for $M = 1, 3, 5$, respectively, result in a triplet $(\pi^*)^2(\delta^*)^2$ ground state. States of multiplicity 1, of the same configuration, are calculated 0.017 au higher in energy than the ground state. States of $M = 5$, on the other hand, lie 0.08 au above the lowest energy triplet. In the same way the description for the other compounds should be interpreted. Oc, occupied orbitals; V, virtual orbitals; $\sigma^*_s$, MO arising from 5s AO on Ru. All other MO are defined in the text or on the corresponding figures.

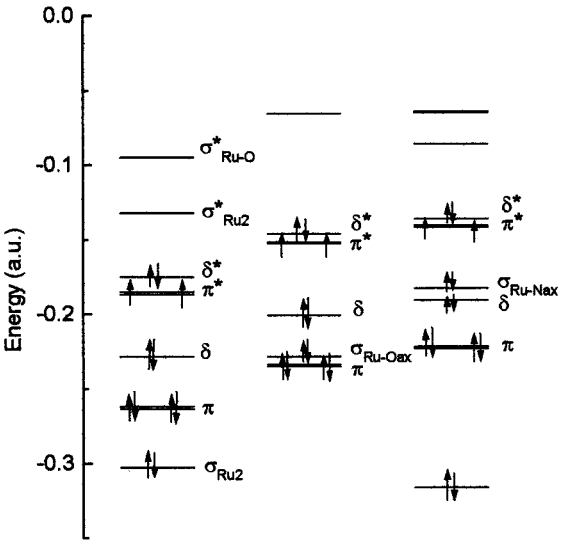


**Figure 3.** Molecular orbital diagram of divalent $Ru_2(O_2CH)_4$ (left), $Ru_2(O_2CH)_4(H_2O)_2$ (middle), and $Ru_2(O_2CH)_4(py)_2$ (right) from DFT computations (eigenvalues in au). Only MO's with high metal contributions have been represented.

**(d) Electronic Spectra.** The UV−visible spectra of the Ru(II,II) carboxylates in solution are dominated by an absorption centered at ca. 450 nm, whose position depends only slightly on the nature of the solvent, provided that it does not coordinate via significant $\sigma$ and $\pi$ bonds, like $CH_3CN$.[10i,13,14,28] This band, that shifts from 460 nm in benzene to 440 nm in oxygen donor solvents, has not been assigned uniquely before. Chisholm and co-workers[13] have considered it consistent with a primarily metal → metal, d-based electronic transition, on the basis of its molar absorbance. In earlier work, Wilkinson et al. proposed, on the basis of the NRC work,[5] a $\pi$(RuO) → $\pi^*(Ru_2)$ assignment, where the $\pi$(RuO) orbital is mainly Ru−O bonding in character, but with an appreciable Ru−Ru bonding contribution as well. Assuming $D_{4h}$ symmetry, the $\pi \rightarrow \pi^*$ ($e_u \rightarrow e_g$) transition is allowed in the z direction, and it is believed to be responsible for the band.

To properly assign the experimental features of the UV−vis spectrum, we have performed MRCI calculations of the INDO/S type, starting from the most stable triplet state of the diaquo complex, a model for oxygen donor solvents. Three reference states were included, and the active space has been defined by 11 orbitals down and 8 orbitals up the Fermi level. Calculations have been done under $D_{2h}$ symmetry. In this way, 204 configurations were generated. The reference states correspond to one $(\pi^*)^2(\delta^*)^2$ and two $(\pi^*)^3(\delta^*)^1$ configurations which are very close in energy. Our calculations confirm the assignment by Chisholm et al. based on experimental grounds,[11,13] predicting a band at 426 nm, that belongs to a *z*-polarized $\pi \rightarrow \pi^*$ transition. Its low intensity is in agreement with its Ru → Ru d−d character. Because of the nature of this transition, the band position will be strongly dependent on the local geometric characteristics of the metal core (Ru−Ru distance).

(28) For example, for $Ru_2(O_2C_4H_7)_4$, we have obtained: in MeOH, $\lambda_{max}$ = 444 nm; EtOH, $\lambda_{max}$ = 442 nm; thf, $\lambda_{max}$ = 444 nm; $CH_2Cl_2$, $\lambda_{max}$ = 446 nm; Ace, $\lambda_{max}$ = 447 nm; $CH_3CN$, $\lambda_{max}$ = 456 nm. These values agree well with those reported for $Ru_2(O_2C_8H_{15})_4$,[13] $Ru_2(OAc)_4(H_2O)_2$,[10i] and $Ru_2(OAc)_4(thf)_2$,[10i] and those measured by us in thf for $Ru_2(O_2C_{12}H_{23})_4$ and $Ru_2(O_2C_{16}H_{31})_4$ (443 nm in both cases). In the solid state, we have obtained $\lambda_{max}$ = 478, 468, and 450 nm for $Ru_2(O_2C_4H_7)_4$, $Ru_2(O_2C_{12}H_{23})_4$, and $Ru_2(OAc)_4(H_2O)_2$ respectively.

It has been experimentally found that axially bonded pyrazine ligands shift the band to 475 nm, increasing significantly its intensity (more than 3 times).[13] This fact has been associated with the influence of the $\pi^*$ LUMO orbital of pyrazine which, being of the appropriate symmetry to interact with the Ru−Ru $\pi^*$ orbital, modifies the characteristics of the transition which turns out to be "metal to ligand" in character, and, therefore, of higher intensity.[13] Our MRCI calculations are in agreement with this assignment. We calculate a band at 463 nm, four times as intense as the band seen for the diaquo complex, which is associated with a metal to ligand charge transfer (MLCT) transition from a $\pi^*$ orbital on the diruthenium core to the $\pi^*$ orbital on the pyrazine ligands. The lowering of the energy, compared to the diaquo species, is also qualitatively explained by the lowering of the $\pi^*$ level due to back-donation. The calculations have also been done under $D_{2h}$ symmetry, including the same reference states as for the diaquo complex, with the active space defined by 20 orbitals down and 15 up the Fermi level. In this way 1280 configurations were generated.

We have also determined experimentally the electronic spectra of the compounds in the solid state. The band that we predicted at 426 nm for the $Ru_2(O_2CH)_4(H_2O)_2$ model compound (experimentally found at ca. 440 nm for $Ru_2(O_2CR)_4$ species in oxygen coordinating solvents)[28] is red shifted 10 nm in the case of $Ru_2(OAc)_4(H_2O)_2$, and 30 to 40 nm in the case of $Ru_2(O_2C_4H_7)_4$ and $Ru_2(O_2C_{12}H_{23})_4$. In all these compounds the axial positions are supposed to be occupied by oxygen atoms: those of the water molecules in the first case, and atoms belonging to neighboring carboxylates in the others. Taking into account that we are dealing with d → d transitions, it is very likely that the shift is derived from a modification of the Ru−Ru distance when the dimers are mutually interconnected defining oligomeric structures. The molecular structures of several di-solvated species are known, but those of the unsolvated species have not yet been determined. For them, the spectroscopic results suggest a little difference in the Ru−Ru distance. In the case of the pyrazine adduct, the electronic spectrum measured in the solid state shows a red shift of the band, relative to the dimer, close to 100 nm. This band is associated, on the basis of our calculations, to a MLCT from the $\pi^*$ on the metal to the $\pi^*$ system of pyrazine, which is also consistent with its high intensity. It has been demonstrated, on the basis of the shifts patterns of the NMR spectra,[13] that direct $\pi$ delocalization of the unpaired electrons occupying the Ru−Ru $\pi^*$ orbital into the aromatic system is occurring in solution, i.e., in the dimeric structure. This effect has also been demonstrated from the INDO/S and DFT descriptions of the MO's. It has to be considered that $\pi$ delocalization will be more effective in the solid state, as the delocalized system becomes longer. This fact offers an explanation to the larger energy shift of the characteristic band. To quantify this effect, we have performed several ZINDO/S calculations on a double-size $[Ru^{II,II}(O_2CH)_4]_2pz_3$ (pz = pyrazine). However, the system is not large enough to account for the effect of delocalization, and therefore is not a proper model of the extended solid.

**(e) Vibrational Spectra.** The solid-state RR spectra of $Ru_2(OAc)_4(H_2O)_2$, $Ru_2(O_2C_4H_7)_4$, $Ru_2(O_2C_{12}H_{23})_4$ (Figure 4), and $Ru_2(O_2C_{16}H_{31})_4$ are dominated by the Ru−Ru stretching band (at ca. 350 $cm^{-1}$), together with the first 4−5 overtones. The existence of a large number of overtones has allowed us to calculate the parameters of the Morse potential hole which are, for the laurate homologue ($n = 12$), $\varpi_e = 350$ $cm^{-1}$ and $x_e\varpi_e = 1.7$ $cm^{-1}$, for the harmonic and anharmonic factors, respectively. In the unsolvated species, the most intense band is in

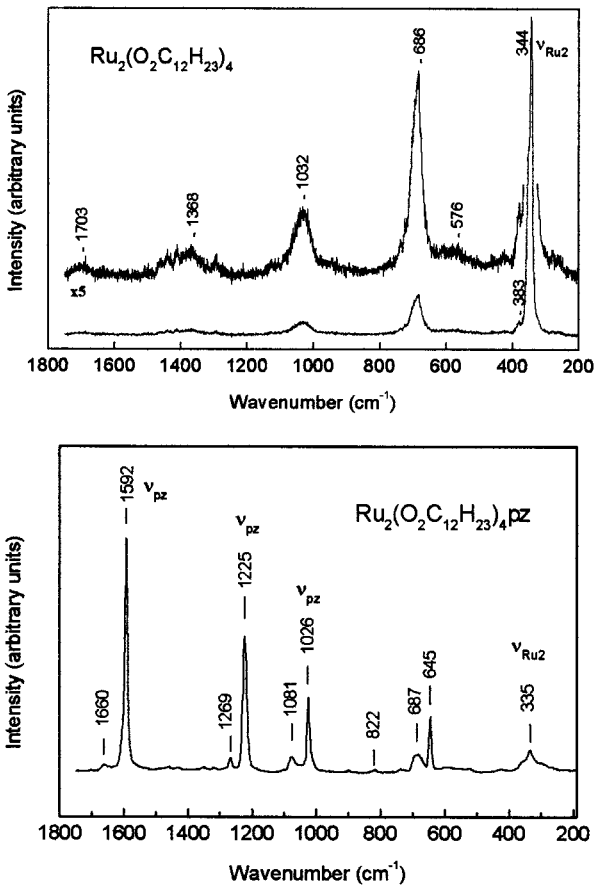


**Figure 4.** Resonance Raman spectra of solid divalent diruthenium tetralaurate, $Ru_2(O_2C_{12}H_{23})_4$ and its pyrazine derivative $Ru_2(O_2C_{12}H_{23})_4$-pz.

fact a doublet, with components at 347 and 355 $cm^{-1}$ (see below). The $Ru_2(OAc)_4(H_2O)_2$ compound exhibits two distinct bands, at 338 and 362 $cm^{-1}$, the first one being absent in the spectra of the unsolvated species. Clark has found a similar result[11b] for the mixed-valent analogue $[Ru_2(OAc)_4(H_2O)_2]BF_4$ and, on the basis of $^{18}O$ isotopic substitution, has attributed the higher energy stretch to a $\nu_{Ru-O}$ mode. However, owing to the intensity ratio of the bands of our divalent compound, we suggest that the most intense band at 362 $cm^{-1}$ could be the $\nu_{Ru-Ru}$ mode.

The pyrazine adduct of the laurate, $Ru_2(O_2C_{12}H_{23})_4pz$, shows a different RR spectrum, also shown in Figure 4, in the sense that the most intense bands are associated to the $\nu_{ag}$ pyrazine modes. In addition, the Ru−Ru stretch shifts to 335 $cm^{-1}$. This result is in agreement and even expands those obtained by Chisholm in their solution RR experiments: the band at 348 $cm^{-1}$ in the "free" $Ru_2(O_2CR)_4$ (solvent is axially coordinated) shifts to 332 $cm^{-1}$ in mixtures of benzene/pyridine or benzene/pyrazine, where the bis-adducts of N-heterocyclic ligands are expected to be the predominant species. The influence of the axial $\pi$-acceptor ligands on the Ru−Ru bond is then confirmed by these experimental results.

The change in the relative intensity of the Raman enhanced bands can be related to the UV/vis spectral changes. Even if we were not able to obtain a complete excitation profile of these bands, it was clear that they were enhanced by green (514.5 nm) or red (614.7 nm) irradiation relative to their intensity when a blue (488.0 nm) laser line was used. The first two lines are closer to the absorption maximum than the latter, and the fact

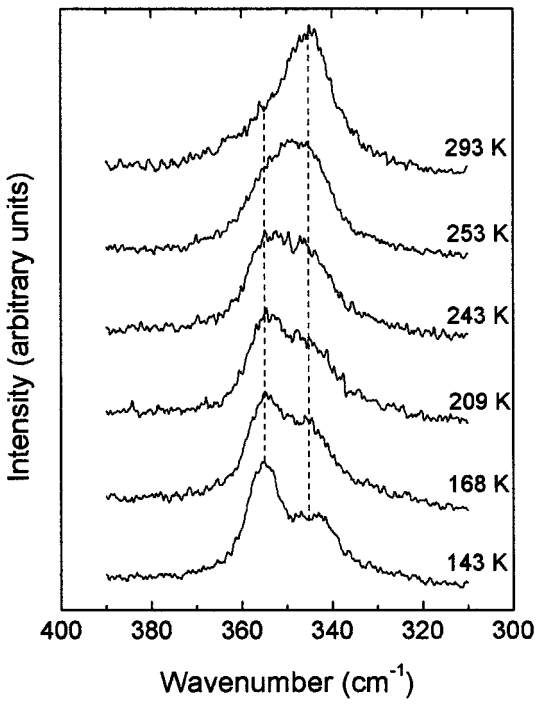


**Figure 5.** Temperature dependence of the $Ru_2$ stretching of $Ru_2(O_2C_4H_7)_4$, as observed in its solid-state resonance Raman spectra.

that this absorption gave rise to an enhancement of the symmetric pyrazine modes supports our previous MLCT assignment.

As stated above, the band at ca. 350 $cm^{-1}$, found in all the divalent unsolvated species studied, is in fact composed by two different bands: one at 347 $cm^{-1}$, and a second one at 355 $cm^{-1}$. Their intensity ratio varies continuously with temperature, as shown in Figure 5 for the case of the butyrate ($n = 4$) derivative. The evolution is completely reversible, and clearly associated with the local heating.[29] Laurate ($n = 12$) and palmitate ($n = 16$) derivatives exhibit the same behavior as the butyrate one. The origin of this thermal behavior is not obvious; one possible explanation is based on the consideration that the ground and first excited electronic states of these compounds might be involved in the band shift. The former (populated at low temperature) might correspond to a Ru−Ru stretching at 355 $cm^{-1}$; the later (which starts to populate as the temperature raises) exhibiting this stretching at 347 $cm^{-1}$, as expected for a slightly weaker Ru−Ru bond. The energy gap between these two configurations, as calculated by ZINDO/S-MRCI, is 0.002 au for both the diaquo tetracarboxylates and the pyrazine complex, in rough agreement with the temperature dependence found for the double-band RR feature.[30]

**Mixed-Valent Compounds. (a) (1) Electronic Structure: ZINDO Calculations.** The $Ru_2^{II,III}$ carboxylates are well characterized in the solid state as complexes with axial aquo or chloride ligands. Following the methodology previously described for the divalent compounds, we have first calculated the axially free $Ru^{II,III}$ complex $[Ru(O_2CH)_4]^+$. In agreement with the experimental evidence, a quartet $(\pi^*)^2(\delta^*)^1$ ground state is predicted (see Table 1 and Figure 6a), with a calculated bond order of 2.5. The electronic configuration we predict, $\sigma\pi\delta\pi^*\delta^*\sigma^*$, is the same as the one in ref 5. It should be mentioned that, according to our calculations, the $\pi$ and $\sigma$ orbitals lie very close in energy, closer than for the divalent case. The relative stability of the $\pi$ and $\sigma$ orbitals can be understood as indicative of a balance between the strength of the interaction between the Ru atoms ($\sigma$ orbital) and the interactions with the oxygen atoms of the carboxylate ligands ($\delta$, $\pi$ orbitals). The strength of the Ru−Ru interaction should be a function of their distance. With no further experimental evidence that may support a different choice, and after the examination of the published structural data,[2,3,8,10−12,14] we have chosen the same distance for both the (II, II) and (II, III) Ru carboxylates, being aware that, having a different bond order, the bond distance might also change, a fact that should be reflected in the energy of the $\sigma$ orbital. Based on this reasoning, we can offer an explanation to the different MO distribution of the antibonding orbitals in the (II,II) and (II, III) ruthenium carboxylates. The fact that the $\delta^*$ orbital is not above the $\sigma^*$ in the latter as it is in the first case can be the result of the larger strength of the Ru−Ru interaction in the (II,III) compounds, which are more tightly bound, and the consequently lower strength of the Ru−carboxylate interaction, which destabilizes to a lesser extent the $\delta^*$ orbital.

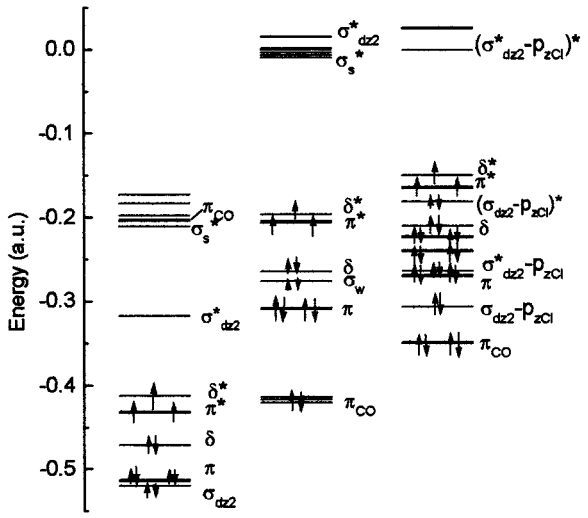


**Figure 6.** MO diagrams ($E$ in au) for mixed-valent $Ru_2(O_2CH)_4^+$ (left), $Ru_2(O_2CH)_4(H_2O)_2^+$ (middle), and $Ru_2(O_2CH)_4Cl_2^-$, (right), after ZINDO/S-MRCI calculations.

**(2) Influence of the Axial Ligands.** The most remarkable effect associated with the interaction of chloride ligands with the $Ru_2(O_2CR)_4^+$ core is the splitting that we calculate for the $\sigma^*_{d_z^2}$ orbital through bonding−antibonding interactions with the $p_z$ orbitals of the chloride ions. The relative position of the $\delta$, $\pi$ orbitals calculated for $[Ru_2(O_2CR)_4Cl_2]^-$ species is the same as in the axially free complex, as it is determined by the interaction with the carboxylate ligands. Its MO distribution (Figure 6) can be represented as $(\sigma_{d_z^2-p_zCl})\pi$ $(\sigma^*_{d_z^2-p_zCl})\delta$ $(\sigma_{d_z^2-p_zCl})^*\pi^*\delta^*(\sigma^*_{d_z^2-p_zCl})^*$. The description is very similar to the one given by NRC, derived from Xα calculations. Our MRCI calculations also predict a $(\pi^*)^2(\delta^*)^1$ ground state of multiplicity 4, $(e_g)^2(b_{2g})^1$ in $D_{4h}$ symmetry (details on the calculation results and procedures are given in Table 1).

(29) Variation of the laser power had the same effect as the external temperature variation. On the other hand, the comparison of the spectra obtained in a "classical" Raman configuration (a powdered sample diluted in KBr) and those registered in the micro-Raman configuration, with a much smaller laser power, confirms the magnitude of the local heating.

(30) Structural reasons, such as a mixture of two kinds of crystalline structures, or the presence of two slightly different kinds of molecules in the crystalline phase might also be invoked. The hypothesis that this thermal behavior can be associated with the crystal−liquid crystal (LC) transition characteristic of long-chain divalent carboxylates is ruled out on the basis of the continuous variation of the intensity ratio with temperature and the fact that the butyrate homologue (which does not exhibit a LC phase) also displays this phenomena.

For the $[Ru_2(O_2CR)_4(H_2O)_2]^+$ species (Table 1), it follows from the ZINDO/S-MRCI analysis that axially bonded water molecules interact—through the $3a_1$ orbital—with the $\sigma^*_{d_{z^2}}$ of the ruthenium core. As shown in Figure 6, the antibonding interaction pushes up the $\sigma^*_{d_{z^2}}$ above the $\sigma^*_s$, locating its bonding counterpart above the $\pi$, to give an electronic configuration $\pi\sigma_w\delta\pi^*\delta^*\sigma^*_s\sigma^*_{d_{z^2}}$. The $\pi\delta$ intercrossing is kept for both the bonding and antibonding groups of orbitals, as it is the result of the interaction with equatorial ligands. In this way, a $(\pi^*)^2$-$(\delta^*)^1$ quartet ground state is predicted.

Axially bonded N-heterocyclic ligands, like pyridine (py) or pyrazine (pz), are characterized by a strong interaction with the Ru atoms of the central core. The ZINDO/S-MRCI calculations show that not only the $\sigma_{d_{z^2}}$ and $\sigma^*_{d_{z^2}}$ are pushed up in energy, the first above the $\delta$ and $\pi$ and the latter above the $\sigma^*_s$, but also the ruthenium $\pi^*$ orbitals interact with the $\pi$ system on the pyrazine, reversing the $\pi^*\delta^*$ ordering, characteristic of the axially free complex, to give a $\pi\delta\sigma_{p_z}\delta^*\pi^*\sigma^*_s\sigma^*_{d_{z^2}}$ electronic distribution.

Because the aromatic rings of the pyrazine ligands are oriented in the plane of the carboxylates, one of the orbitals (the one in the plane) supports most of the interaction with the pyrazine $\pi$ system, an effect that is reflected in a splitting of the $\pi$'s. This effect does not become so evident in the $Ru^{II,II}$ complexes, where the through-chain interactions are less important. The symmetry of the molecule is lowered to $D_{2h}$ through coordination with the aromatic rings, and the definition of the $\pi$ orbitals that we are using is only formal, based on the atomic orbitals to which they belong. According to the MRCI calculations (Table 1), the ground state is a quartet $(\delta^*)^1(\pi^*)^2$, which is 0.02 au more stable than the $(\delta^*)^1(\pi^*)^2$ doublet.

Similar calculations have been performed for the pyridine adduct. The main difference between both complexes is related to the orientation of the aromatic rings relative to the planes defined by the carboxylate groups.[12b] Whereas the pyrazine ligands are oriented with the rings lying in the plane of the carboxylates, the pyridine ligands are defining an angle close to 45° with those planes. The MO description is largely obscured by this fact. Nevertheless, we calculate a quartet $(\delta^*)^1(\pi^*)^2$ ground state, which is 0.02 au more stable than the $(\delta^*)^1(\pi^*)^2$ doublet.

In the case of the hexacarboxylates, $[Ru_2(O_2CH)_6]^-$, the interaction with the equatorial ligands, which destabilizes the $\delta$ orbitals, is partially compensated by the interaction with the axial ligands, which destabilizes the $\pi$'s. This results in a $\pi\delta\sigma_{Oax}\delta^*\pi^*\sigma^*_s\sigma^*_{d_{z^2}}$ MO distribution, with the set of ligand orbitals very close in energy. The most relevant characteristic is the destabilization of the $\sigma^*$ orbital through interactions with the axial ligands. The calculated ground state is a quartet $(\delta^*)^1(\pi^*)^2$. The first excited states involve the same $\delta^*/\pi^*$ orbitals (Table 1); states of higher multiplicity ($M = 6$), associated with the promotion of an electron to the $\sigma^*_{d_{z^2}}$ orbital, are 0.8 au above the ground state.

For these compounds, characterized by the presence of the same ligands in both the axial and equatorial positions, the effect of choosing a different model, where only one of the axial positions is bonded to a carboxylate whereas the other remains free, has been analyzed. The MO distribution does not change, provided the orbital space is appropriately defined in the cahf calculations. However, the interaction with only one axial ligand reinforces the Ru−Ru $\sigma$ interaction, leading to a lower destabilization of the $\sigma_{d_{z^2}}$ orbital. This effect is even more remarkable in the complex with chloride axial ligands, where the relative position of the $\sigma^*_s$ and $\sigma^*_{d_{z^2}}$ orbitals is interchanged when either one or two axial ligands are considered in the model.

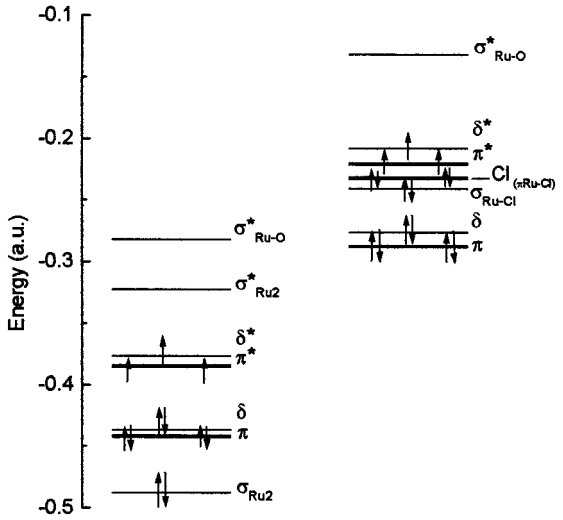


**Figure 7.** MO scheme of $Ru_2(O_2CH)_4^+$ (left) and $Ru_2(O_2CH)_4Cl$ (right), after DFT calculations.

**Table 2.** $\lambda_{max}$ of the Mixed-Valent $Ru_2(O_2CR)_4X$ Compounds in Different Media (Values Averaged for Several Chain Lengths in Each Entry)

| $X^-$ | MeOH | EtOH | *n*-PrOH | $CH_2Cl_2$ | $Et_2O$ | $CH_3CN$ | solid phase |
|---|---|---|---|---|---|---|---|
| $Cl^-$ | 428 ± 1 | 431 ± 2 | 436 ± 1 | 452 ± 1 | 466 ± 1 | 457 ± 1 | 478 ± 3 |
| $RCO_2^-$ | 427 ± 2 | 430 ± 2 | − | 442 ± 2 | − | 428 ± 1 | 445 ± 3 |

**(b) Electronic Structure: DFT Calculations.** The MO diagram of the $Ru_2(O_2CH)_4^+$ species is shown in Figure 7. The $\pi^*$ and $\delta^*$ levels are interchanged, a result that is in agreement with the conclusions of the NRC-X$\alpha$ calculations[5] and with those derived from the ZINDO/S-MRCI calculations as well. The ground state is therefore a quadruplet state, arising from a $(\pi^*)^2(\delta^*)^1$ valence configuration. The influence of an axially coordinated chloride anion is also represented in Figure 7 for the $Ru_2(O_2CH)_4Cl$ species. As it has been previously described in relation to the MRCI results, the $p_z$ chlorine AO interacts with the $\sigma$ and $\sigma^*$ (Ru−Ru) MO's and a $\sigma$(Ru−Cl) component appears below the $(\pi^*,\delta^*)$ set. Another component of the interaction is a $Cl(3p_x, 3p_y)$ interaction with the $\pi^*$ orbitals, noted as a $\pi$(Ru−Cl) bond.

**(c) Electronic Spectra.** The UV/vis/NIR absorption spectra of short aliphatic chain mixed-valence diruthenium carboxylates have been particularly well studied between 1980 and 1988.[11] Here we extend these studies to the long-chain homologues corresponding to both the chloride ($Ru_2(O_2CR)_4Cl$) and the carboxylate ($Ru_2(O_2CR)_5$) series.

The UV/visible spectra of all the members included in our study exhibit a prominent band near 450 nm, which has previously been assigned to a $\pi(RuO) \rightarrow \pi^*(Ru_2)$ ($6e_u \rightarrow 6e_g$) transition on the basis of the composition of the MO's obtained by X$\alpha$ calculations.[5,11] Some authors, however, have suggested that it can belong to a pure metal−metal $\pi \rightarrow \pi^*$ transition, on the basis of the intensity of the band and the resonance Raman data.[11d,13] The position of the band is fairly dependent on the chemical environment. Table 2 collects the average values for several members of each series, corresponding to chloride and carboxylate axial ligands in different environments.[14]

The values obtained for the chloride compounds can be divided into three categories: those measured using an alcohol as solvent, whose maxima appear close to 430 nm, those

measured in $CH_2Cl_2$, $Et_2O$, and acetonitrile (ca. 460 nm) and those measured in the solid state (480 nm). In the first series, where the chloride is supposed to be fully dissociated, the chromophore is a $[Ru_2(O_2CR)_4(S)_2]^+$ cation, with the cationic dimeric core solvated by two alcohol molecules (S). In the solid-state spectra, the $[Ru_2(O_2CR)_4]^+$ cations are coordinated in both axial positions by chloride counterions (the $\lambda_{max}$ values are similar to those found for $[Ru_2(O_2CR)_4Cl_2]^-$ species, i.e., 470 nm).[11d] In low polar solvents, the complexes are weakly dissociated, and we may assume that the species present in solution are molecules coordinated by only one chloride in an axial position; the values obtained are indeed halfway between the two extreme situations just described.

Similar comments apply to the case of the pentacarboxylate series: in alcoholic solutions, the maximum wavelength is still at ca. 430 nm, as in the case of the chloride series, as the chromophoric species, $[Ru_2(O_2CR)_4(S)_2]^+$ (S = alcohol), is the same, and the anion does not play any role in the absorption process. The values obtained in the solid state spectra of the pentacarboxylates, where both axial positions of each molecule are occupied by oxygen atoms from the carboxylate anions, are close to 445 nm, clearly different from those obtained in solid state for the chloride analogues, as different axial substituents are implied. Moreover, values obtained in dichloromethane solution are similar to those found in the solid state, consistently with a weak dissociation in this solvent, the absorption species being always axially coordinated by at least one oxygen atom. These results are in agreement with a recent work on $Ru_2(O_2CR)_4L_2^+$ adducts, where the position of the band was found to be slightly dependent on the donor number of L for oxygenated axial ligands.[8]

We have used our $[Ru_2(O_2CH)_4L_2]^+$ model to analyze, by means of ZINDO/S-MRCI calculations, the dependence on the environment of the UV−visible spectra. According to the previous description, water molecules have been used as axial ligands in order to simulate the effect of oxygenated axial ligands (solvent or others). Chloride axial ligands have been used, on the other hand, to simulate the solid environment.

The calculations for the compound with axially bonded water molecules have been done under $C_{2v}$ symmetry, starting from the most stable quartet, for a MRCI space that includes 10 orbitals up and 10 down the Fermi level, giving rise, in this way, to 250 configurations. The band that experimentally develops around 430 nm (Table 2) is calculated at 409 nm and associated to a $\pi_{Ru} \rightarrow \pi^*_{Ru}$ (d → d) transition, with some contribution of $\delta_{Ru} \rightarrow \pi_{CO}$ MLCT. The assignment is, therefore, similar to the one found for the (II,II) dimer. Because of the nature of the transition that originates the band, its position is strongly dependent on the Ru−Ru distance that determines the splitting of the d orbitals, as it has been shown by some recent experimental results[8] as well as by our own calculations. In fact, the calculations reported here correspond to a Ru−Ru distance 0.05 Å longer that the one for the (II,II) dimers. This seems to be at variance with the higher bond order of the mixed valent species than the divalent compounds. It is, however, in agreement with the Ru−Ru stretching frequencies which, contrary to what one might expect, are higher in the divalent species, with bond order of 2, than in the cationic species, with bond order of 2.5.[13] The calculations for the molecule with axially bound chloride ligands have been done under $D_{2h}$ symmetry, starting also from the most stable quartet, and working on a MRCI space defined by 10 orbitals down and 8 up the Fermi level. 270 configurations result, in this way, from the calculations. The band that develops experimentally at 475 nm for a calculated value of 464 nm, corresponds to the same assignment as previously discussed for the diaquo complex, and also to the same shift in the Ru−Ru interatomic distance.

**Table 3.** $Ru_2$ Stretching Wavenumber (in $cm^{-1}$) Measured in the Solid State RR Spectra for Several Mixed-Valent Diruthenium Complexes

| compound | $\nu(Ru_2)$ |
|---|---|
| $Ru_2(O_2C_2H_3)_4Cl$ | 329 |
| $Ru_2(O_2C_4H_7)_4Cl$ | 333 |
| $Ru_2(O_2C_5H_9)_4Cl$ | 333 |
| $Ru_2(O_2C_8H_{15})_4Cl$ | 333 |
| $Ru_2(O_2C_{16}D_{31})_4Cl$ | 332 |
| $Ru_2(O_2C_{16}H_{31})_4DOS$ | 347 |
| $Ru_2(O_2C_8H_{15})_5$ | 347 |
| $Ru_2(O_2C_{12}H_{23})_5$ | 350 |
| $Ru_2(O_2C_{16}D_{31})_5$ | 354 |

These results show that the axial coordination has a nonnegligible influence on the energy of the transition. Indeed, we have shown that this energy is higher when the $Ru_2(O_2CR)_4^+$ species is axially coordinated by oxygen donor ligands, as compared to chloride anions.

**(d) Vibrational Spectra.** Focusing our attention on the Ru−Ru stretching vibration, we have studied the RR spectra of several compounds belonging to both the $Cl^-$ and $RCO_2^-$ series. A dodecyl sulfate derivative, namely $Ru_2(O_2C_{16}H_{31})_4$-DOS has also been studied. As in the case of the divalent compounds, the spectra are dominated by the Ru−Ru stretching band and its overtones, even if some metal−ligand and intraligand modes are also detectable. This fact has been previously shown by Clark and co-workers in their work on short-chain chlorocarboxylates.[11b] The values of $\nu(Ru_2)$ are collected in Table 3. (Table S1 also includes the overtones of $\nu(Ru_2)$; the RR spectra of $Ru_2(O_2C_8H_{15})_4Cl$, $Ru_2(O_2C_{16}H_{31})_4DOS$, and $Ru_2(O_2C_{12}H_{23})_5$ are included in Figures S1, S2, and S3, respectively, as illustrative examples.)

The frequency of the Ru−Ru vibration in the chloro-complexes is 333 ± 1 $cm^{-1}$. This value is in agreement with the values from the literature for the formiate (339 $cm^{-1}$), acetate (327 ± 1 $cm^{-1}$), hydrated acetate (326 $cm^{-1}$), propionate (337 ± 1 $cm^{-1}$), and butyrate (330 ± 2 $cm^{-1}$) homologues. In the pentacarboxylate series, the $\nu(Ru_2)_1$ vibration appears at 350 ± 4 $cm^{-1}$, a value close to that found for the dodecyl sulfate derivative (347 $cm^{-1}$). These values seem to depend on the nature of the donor atom of the axial ligand, as it was the case for the electronic transitions. For oxygen-containing ligands, the values are very similar to those found for the divalent species and not slightly higher than them, as it has been previously stated.[13] This fact is in agreement with the very similar Ru−Ru distances characteristic of both the (II,II) and (II,III) derivatives, and with the electronic configurations that have been proposed.

**(e) Magneto-Structural Correlation in Mixed-Valent Chlorocarboxylates.** As reported elsewhere,[7d] a correlation has been observed between the magnitude of an antiferromagnetic (AF) intermolecular interaction and the Ru−Cl−Ru angle in the alternating chains $-Ru_2(O_2CR)_4-Cl-Ru_2(O_2CR)_4-Cl-...$ in the crystalline phase. As the angle approaches 180°, the AF interaction was found to increase significantly. On the basis of the well-known theory[31] that relates the AF intermolecular coupling to the amount of overlap between magnetic orbitals,

(31) (a) Hay, P. J.; Thibeault, J. C.; Hoffmann, R. *J. Am. Chem. Soc.* **1975**, *97*, 4884. (b) Kahn, O.; Briat, B. *J. Chem. Soc., Faraday Trans. 2* **1976**, *72*, 268. (c) Kahn, O. In *Magneto-Structural Correlations in Exchange Coupled Systems*; Willet, R. D., Gatteschi, D., Kahn, O., Eds.; Nato ASI Series 37; D. Riedel Publishing Co.: Dordrecht, 1984.

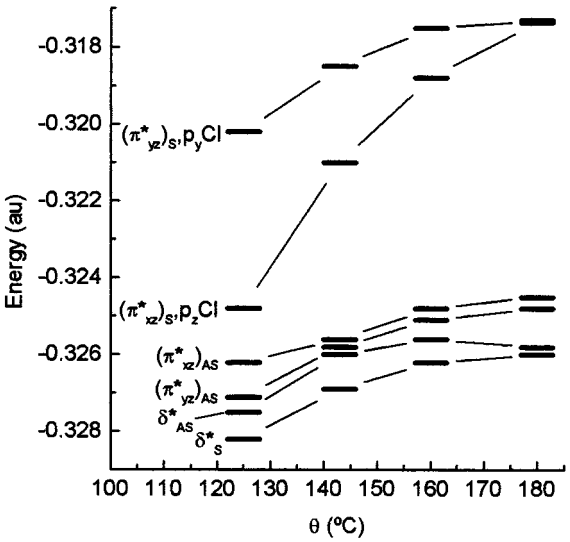


**Figure 8.** Evolution of the energy of the magnetic orbitals (*E*, au) as a function of the Ru−Cl−Ru angle ($\theta$, deg).

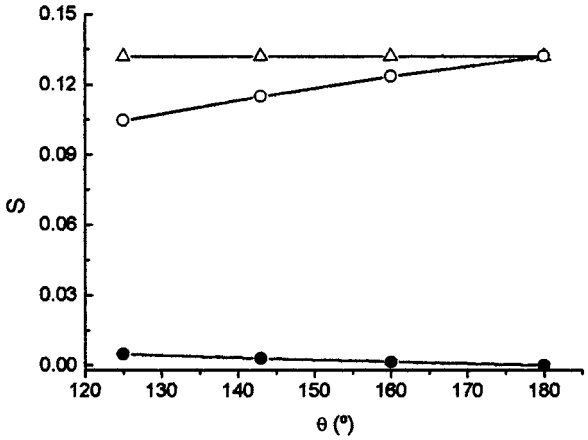


**Figure 9.** Evolution of overlaps with the Ru−Cl−Ru angle ($\theta$, deg) for the following combinations: $\Phi_A$ ($\pi^*_{xz}$, $p_z$) (●); $\Phi_S$ ($\pi_{xz}$, $p_x$) (○); $\Phi_S$ ($\pi^*_{yz}$, $p_y$) (△).

we qualitatively examined its evolution as the Ru−Cl−Ru changes.[7d] We concluded that there is an overall increase of the overlap when the system is approaching a linear structure, i.e., an angle of 180°. Three combinations of magnetic orbitals were found to yield significant contributions, namely the symmetric ones $(\pi^*_{yz}, 3p_y)_S$, $(\pi^*_{xz}, 3p_x)_S$ and the antisymmetric $(\pi^*_{xz}, 3p_z)_A$ contribution.[7d] When going to the linear conformation, the overlap of the orbitals in the combination $(\pi^*_{yz}, 3p_y)_S$ was found to be constant, whereas the second one, $(\pi^*_{xz}, 3p_x)_S$, was found to increase to reach the same value as the first, and the third one, $(\pi^*_{xz}, 3p_z)_A$, was found to decrease to 0.

The DFT computations described here provide more quantitative information about the overlap of the various 3p Cl and $\pi^*$(Ru−Ru) combinations. The model system $[Ru_2(O_2CH)_4-Cl-Ru_2(O_2CH)_4]^+$ has been considered for several values of the Ru−Cl−Ru angle $\theta$, namely, $\theta = 125°$, 142°, 160°, and 180°. The energies of the resulting antisymmetric (AS) and symmetric (S) magnetic orbitals, which describe the six unpaired electrons of the system, are represented in Figure 8 as a function of the angle $\theta$. One interesting feature is the splitting of the $(\pi^*_{yz}, 3p_y)_S$ and $(\pi^*_{xz}, 3p_x)_S$ orbitals, which decreases when $\theta$ approches 180°, as the $\pi^*_{yz}$ and $\pi^*_{xz}$ become degenerate when the geometry becomes linear.

The significant overlap values given by the computations are represented in Figure 9, as a function of the angle $\theta$. It is clear that the evolution is the same as the one predicted by our previous qualitative arguments.[7d] We may therefore expect an increase of the overall overlap of the magnetic orbitals in the linear structure, thus leading to the observed increase of AF coupling between the dimeric units.

## Conclusions

The quantum chemical calculations presented in this article have demonstrated their accuracy for the interpretation of both the electronic structure and UV−vis spectra of divalent and mixed valent Ru carboxylates. Both the structural and spectroscopic (UV/vis, RR) similarities, as well as the different MO distributions calculated for them, indicate that a delicate balance between the Ru−Ru and Ru−O(equatorial carboxylate) bond strengths contributes to the determination of their properties.

The influence of the nature of the axial ligands on the electronic structure of these compounds is also significant. It has been found to depend both on its $\sigma$ donor and $\pi$ donor and acceptor character. Particularly interesting is the prediction of a quintuplet ground state for the unligated divalent $Ru_2(O_2CR)_4$ species derived from the ZINDO/S-MRCI calculation, which was not confirmed by DFT calculations. Experimental work on the synthesis and spectroscopic analysis of such a derivative is strongly recommended.

Among the UV−vis spectroscopic features that have been assigned, the interpretation of the 430 nm band has to be highlighted, as it has been a subject of controversy for a long time, in relation to its d → d or LMCT nature, for both the divalent and the mixed valent compounds.

The calculations have also allowed us to explain the experimental magnetic behavior of the axially ligated divalent derivatives, which appears to be a consequence of the $(\pi^*)^2(\delta^*)^2$ ground-state configuration. This configuration, that has been previously inferred by Cotton et al, has been corroborated now on the basis of both DFT and ZINDO calculations.

In addition to its success in the analysis of the physicochemical properties of the dimeric compounds, it can be anticipated that the methodology presented in this article would be useful also in the study of oligomeric and polymeric systems, built up on the dimeric units. The successful quantitative interpretation given by DFT for the intermolecular AF exchange in mixed-valent carboxylates, previously analyzed on a qualitative basis, define the first step. Research in this direction is presently being performed in our labs and will be the subject of a forthcoming paper.

**Acknowledgment.** We thank Gérard Sagon (LASIR, Thiais) for helping us in some of the RR experiments, as well as Dr. Robert Subra (Université Joseph Fourier, Grenoble) and Dr. A. B. P. Lever (York University) for their interesting comments on the interpretation of some experimental results. Financial support from the Universities of Buenos Aires (Grant UBACyT EX117) and La Plata, as well as from the Fundación Antorchas and Secyt-Ecos (Grant for International Cooperation A97E08) is acknowleged. G.E. and F.D.C. are members of the research staff of Conicet.

**Supporting Information Available:** A table containing the wavenumber of the first overtones of the Ru−Ru stretching vibrations for 9 different compounds, as well as 3 figures showing the RR spectra of mixed-valent diruthenium carboxylates with different anions: $Cl^-$, DOS, $RCO_2^-$. This material is available free of charge via the Internet at http://pubs.acs.org.

IC981098+